Dependence of the L-Alanyl-L-Alanine Conformation on Molecular Charge Determined from Ab Initio Computations and NMR Spectra

Vladimír Sychrovský,* Miloš Buděšínský,* Ladislav Benda, Vladimír Špirko,* Zuzana Vokáčová, Jaroslav Šebestík, and Petr Bouř*

Institute of Organic Chemistry and Biochemistry, Academy of Sciences, Flemingovo nám. 2, 16610, Prague 6, Czech Republic

Received: August 15, 2007; In Final Form: October 21, 2007

The L-alanyl-L-alanine (AA) molecule behaves differently in acidic, neutral, and basic environments. Because of its molecular flexibility and strong interaction with the aqueous environment, its behavior has to be deduced from the NMR spectra indirectly, using statistical methods and comparison with ab initio predictions of geometric and spectral parameters. In this study, chemical shifts and indirect spin−spin coupling constants of the AA cation, anion, and zwitterion were measured and compared to values obtained by density functional computations for various conformers of the dipeptide. The accuracy and sensitivity of the quantum methods to the molecular charge was also tested on the (mono)-alanine molecule. Probable AA conformers could be identified at two-dimensional potential energy surfaces and verified by the comparison of the computed parameters with measured NMR data. The results indicate that, whereas the main-chain peptide conformations of the cationic (AA^+) and zwitterionic (AA^{ZW}) forms are similar, the anion (AA^-) adopts also another, approximately equally populated conformer in the aqueous solution. Additionally, the NH_2 group can rotate in the two main chain conformations of the anionic form AA^-. According to a vibrational quantum analysis of the two-dimensional energy surfaces, higher-energy conformers might exist for all three charged AA forms but cannot be detected directly by NMR spectroscopy because of their small populations and short lifetimes. In accord with previous studies, the NMR parameters, particularly the indirect nuclear spin−spin coupling constants, often provided an excellent probe of a local conformation. Generalization to peptides and proteins, however, has to take into account the environment, molecular charge, and flexibility of the peptide chain.

Introduction

NMR spectroscopy has a long history in the conformational analyses of peptide structures.[1,2] Empirical correlations of chemical shifts and nuclear spin−spin coupling constants (*J*-coupling) with the geometry were originally used to discriminate helical and sheetlike peptides and subsequently were extended to protein studies.[3−5] The possibility to calculate the NMR parameters for larger molecules with reasonable precision has lately provided an additional basis for the interpretation of the experiment, which consequently facilitated the verification of various conformational models. Particularly, the analytical approaches to chemical shifts[6] and the coupling constants[7−9] within the density functional theory (DFT) speeded up the computations and facilitated the conformational studies of interesting peptide systems.[10,11] The computations improved, for example, the empirical Karplus relations between the spectra and the structure.[12,13] However, peptide flexibility, solvent effects, and local vibrational motions have to be taken into account in accurate modeling.[14]

The dependence of the L-alanyl-L-alanine (AA) conformation on molecular charge studied in this work thus provides additional information about the behavior of the peptide chain in various pH conditions as well as about the accuracy and validity of current simulation techniques. NMR properties of charged and zwitterionic peptides themselves are notoriously difficult to calculate[15] mainly because of the electronic charge concentration requiring a large basis set and because of the strong interaction with the environment, in most cases with water.[16] The three AA forms also provide an experimentally well-accessible example of a simple molecular mechanical system controllable by pH. Therefore, we find it interesting to analyze in detail the two-dimensional potential energy surface and account for possible vibrational quantum effects.[17]

In the second part of this work, we use the statistical comparison of the experimental and computed chemical shifts and spin−spin coupling constants developed previously for the AA zwitterion.[11] The ability of the computation to discriminate between various charged forms is tested on the alanine molecule (A) labeled with stable ^{15}N and ^{13}C isotopes, where the conformational problem is simpler than in AA. The influence of the charge on the molecular potential energy surface, expressed as a function of the main-chain peptide torsion angles (φ, ψ), is computed with the inclusion of a continuum solvent correction. It appears that the pH (charge) change stabilizes a new anion (AA^-) conformer and that the conformational equilibrium can be proven from the NMR data. The quantum vibrational analysis predicts also other well-defined conformers, which, however, are neither significantly populated under normal conditions nor can be observed directly by NMR due to their short lifetimes.

Experimental Section

Isotopically labeled L-alanine (^{13}C,98%; ^{15}N,98%) was purchased from Stable Isotopes, Inc., whereas the nonlabeled AA

* To whom correspondence should be addressed: E-mail: vladimir.sychrovsky@uochb.cas.cz (V.S.), budes@uochb.cas.cz (M.B.), vladimir.spirko@marge.uochb.cas.cz (V.S.), bour@uochb.cas.cz (P.B.).

10.1021/jp076557j CCC: $40.75
Published on Web 01/03/2008

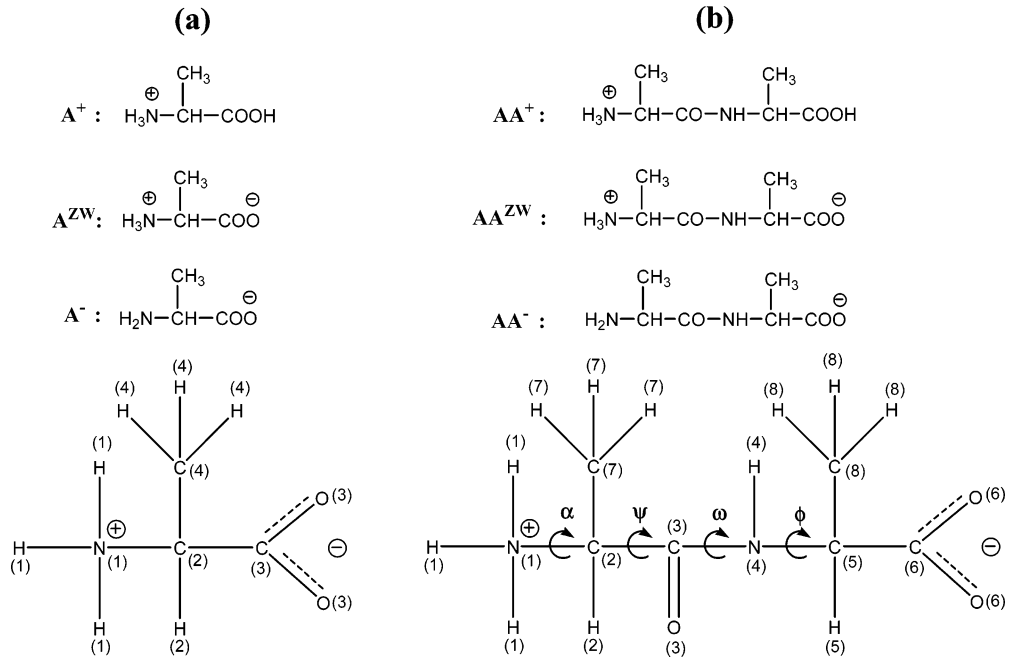

Figure 1. The ionic forms and symbols used for L-alanine (a) and AA (b). The numbering of the atoms for the definition of NMR parameters is shown in zwitterionic forms of both molecules. In addition to standard peptide torsion angles (ϕ, ψ, ω), we have introduced the angle α as the average angle of the two amine hydrogen $-$(C3$-$C2$-$N1$-$H1) torsion angles (for the NH_2 residue in AA^-).

was purchased from Sigma. The synthesis of labeled AA is described elsewhere.[11] NMR spectra of labeled alanine (A^+, A^-, A^{ZW}), natural AA (AA^+, AA^-, AA^{ZW}), and labeled AA^{ZW} were measured with Fourier transform (FT) NMR spectrometers Varian UNITY-500 and Bruker AVANCE-500 (^{1}H at 500 MHz, ^{13}C at 125.7 MHz, ^{15}N at 50.7 MHz, ^{17}O at 67.8 MHz) in D_2O and/or in the mixture H_2O/D_2O (9:1). The solution pH was varied by additions of 2 M HCl (pH $\approx$ 2) and NaOH (pH $\approx$ 12) solutions. For these pH values, the AA peptide exists exclusively in the AA^+ and AA^- forms, respectively, which was confirmed by measuring of the NMR titration curves (provided in the Supporting Information (SI), together with relevant p*K* constants for A and AA). The zwitterionic forms were obtained by dissolving the compounds in distilled water without any buffer. All spectra were measured at room temperature. Chemical shifts were referenced either to internal (DSS for ^{1}H and ^{13}C and H_2O for ^{17}O, but the oxygen is not discussed in this work) or external (nitromethane in the capillary for ^{15}N) standards. The structural assignment of the hydrogen and carbon chemical shifts was achieved using homonuclear and heteronuclear two-dimensional techniques with pulse field gradients (2D-^{1}H,^{1}H-PFG-COSY, ^{1}H,^{13}C-PFG-HSQC, and 2D-^{1}H,^{13}C-PFG-HMBC) in D_2O. The solvent mixture H_2O/D_2O (9:1) was used to observe the signals of NH and NH_3^+ protons. Only the couplings of amide NH could be observed in this mixture because of the fast exchange rate of amine NH_3^+ protons with water. The *J*(H,H) values were determined from the 1D-^{1}H NMR spectrum and the *J*(C,H) couplings from the non-decoupled 1D-^{13}C NMR spectrum. A series of selective ^{1}H-decoupled ^{13}C NMR spectra was used to assign individual *J*(C,H) couplings. The labeled ^{15}N and ^{15}N,^{13}C AA samples were used mainly in order to obtain *J*(N,H), *J*(N,C), and *J*(C,C) coupling constants using the 1D-^{1}H and ^{13}C NMR spectra, the 1D-^{13}C-INADEQUATE (Incredible Natural Abundance Double Quantum Transfer Experiment), and the 2D-^{1}H,^{15}N-PFG-HMBC spectra.

Calculations. The GAUSSIAN software[18] was used for the quantum chemical computations. The torsion angles φ and ψ (Figure 1) were varied with 30° steps, and for each of the resultant $12 \times 12 = 144$ geometries, all the remaining coordinates were fully relaxed by energy minimization. The angle ω was initially set to 180° so as to maintain the *trans*-peptide bond, because the experimental data do not suggest a presence of the *cis*-conformer. In the scans, the relaxed ω angle deviated from 180° by less than ~5°. The BPW91[19] functional and the standard Pople-type 6-311++G** basis were used with the PCM solvent model for water.[20] For the anion AA^-, three scans were performed (3×144 points), taking into account three initial orientations ($\alpha = -120$, 0, and 120°) of the NH_2 group. For this purpose, we defined the angle α as an average of the two amine hydrogen $-$(C3$-$C2$-$N1$-$H) angles. The geometries of the local minima located on the resultant surfaces were fully optimized without any constraints. The scan of the zwitterion mimics previous computations done with smaller grid steps.[11] For control computations, other potential energy scans were done in a vacuum for AA^+ and AA^- (AA^{ZW} is not stable without solvent), and local minima geometries were reoptimized at the MP2[21]/6-311++G** level of approximation.

For the grid points and local minima geometries, the NMR shielding tensors and the indirect NMR spin$-$spin coupling constants were calculated. The default gauge-invariant atomic orbital (GIAO)[22] method was used for the shieldings to prevent their origin dependence. For the *J*-couplings, all four important terms[7,23] were included in the analytical coupled-perturbed DFT computation. For the shieldings and *J*-couplings, we used the B3LYP functional[24] with the IGLOII or IGLOIII bases,[25] which are believed to be well-suited for computations of the NMR properties.[8] In all cases, the same PCM solvent model was applied. With the same method, the NMR parameters were calculated for the anion, cation, and zwitterion of (mono)-alanine in equilibrium geometries. Chemical shifts were related to standard molecules (DSS for ^{1}H and ^{13}C, nitromethane for ^{15}N, water for ^{17}O, same as in ref 11).

The quantum and dynamical effects of the torsional motions involving the angles (φ, ψ) were studied using an approximate Hamiltonian described in full in ref 11, where the potential was obtained by fitting of the computed two-dimensional surfaces, and the kinetic part was expressed in the curvilinear angular

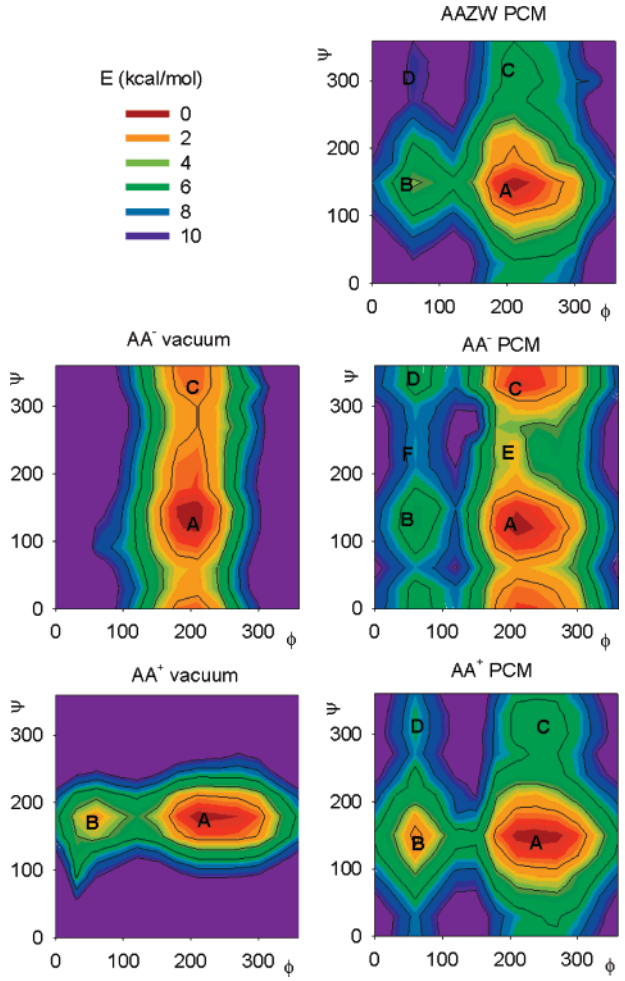

Figure 2. Contour plots of the computed (BPW91/6-311++G**) potential energy surfaces of the three AA forms. By default, the PCM solvent model was applied (right-hand side); for the AA^+ and AA^- forms stable in a vacuum, the dependencies without the solvent are shown on the left. Approximate positions of local minima are marked by the capital letters. To avoid splitting of the minimum well, the angles are plotted within the positive (0, 360°) interval instead of the usual (−180, 180°) range.

coordinates.[26] The eigenvalue vibrational problem $H\Psi = E\Psi$ was solved variationally in basis set functions expressed as products of the eigenfunctions of the corresponding uncoupled one-dimensional Schrödinger equations. The one-dimensional functions were determined numerically using the Numerov−Cooley integration procedure[27] and used for averaging the NMR parameters. The averaging, however, did not bring significant corrections with respect to the overall accuracy and is not discussed further. The lifetimes of selected localized excited vibrational states were estimated from simplified one-dimensional modeling.[11,28]

Results and Discussion

AA Conformers. The calculated adiabatic energy dependencies on the φ and ψ torsion angles are presented in Figure 2. Apparently, the energy profiles of the three hydrated forms exhibit several similarities. The global minimum **A** is associated with comparable angle values for all cases (see Table 1 for details). The similarity of the AA^{ZW} and AA^+ surfaces is the most obvious. However, the protonation of AA^{ZW} makes the resultant cation (AA^+) more flexible with respect to the φ rotation, and the potential well is elongated along this coordinate. The MP2 method provides an equilibrium value of the φ angle (−151°, see Table 1) even significantly shifted from the DFT angle of −121°. For AA^+, the local energy minimum **B** deepens when compared to the other forms, but its relative energy of 1.4 kcal/mol (cf. Table 1) and narrow potential well probably still prevent a significant population of this conformer in the sample. Obviously, the least probable is an occurrence of the other two, **C** and **D** conformers of AA^{ZW} and AA^+.

The energy surface of the anion (AA^-, the middle of Figure 2) is different. Whereas the geometry of the lowest-energy **A** conformer is very close to that of the zwitterion, the minimum well **C** significantly broadens, and its energy is comparable with the global minimum **A**. Additionally, new, very shallow minima (**E**, **F**) appear for the anion; these are, along with the **B** and **D** extremes, not populated due to their high relative energies. For **C**, however, the computed relative energy (0.4 kcal/mol, Table 1) is probably comparable with the computational error and suggests a significant presence of this conformer in the sample at room temperature.

The more complicated behavior of the anion AA^- stems predominantly from the directional and ambivalent binding properties of the NH_2 group. The nitrogen electron lone pair can make an internal hydrogen bond to the amide hydrogen, or the NH_2 protons can be bonded to the carbonyl oxygen. This is documented in Figure 3, where for a fixed value of $\varphi = -150°$ the energy dependence on the ψ angle is plotted. Although detailed three- or more dimensional energy scans are currently not feasible, the coupling of the α, ψ, and φ torsional motions

TABLE 1: Computed (BPW91/PCM/6-311++G) Geometries and Relative Conformer Energies of the Three Charged AA Forms[a]**

	AA^+			AA^{ZW}			AA^-			
conformer	ψ	φ	E	ψ	φ	E	α	ψ	φ	E
A	149	−121	0.0	147	−153	0.0	−2	127	−152	0.0
A′							118	128	−151	0.8
A″							−125	119	−150	1.9
A[b]	178	−159					−11.3	138	−160	
A[c]	150	−151		146	−158		−13.1	133	−157	
A[d]	169	−160					−2.5	139	−160	
B[e]	150	60	1.4	150	66	3.6	−3	135	63	4.3
C	−55	−127	5.1	−51	−150	5.1	−136	−19	−152	0.4
C′							145	8	−147	0.8
C″							9	−21	−150	1.4
D	−55	53	6.3	−48	64	9.2	−138	−16	63	5.0
E							5	−105	−154	2.7
F							7	−116	61	6.9

[a] Torsion angles (φ, ψ, α) are given in degrees and the relative energies (E) in kcal/mol. [b] BPW91, gas phase. [c] MP2, PCM. [d] MP2, gas phase. [e] Calculated lifetimes of this conformer are approximately 1, 6−10, and 0.7 ms for AA^+, AA^{ZW}, and AA^-, respectively.

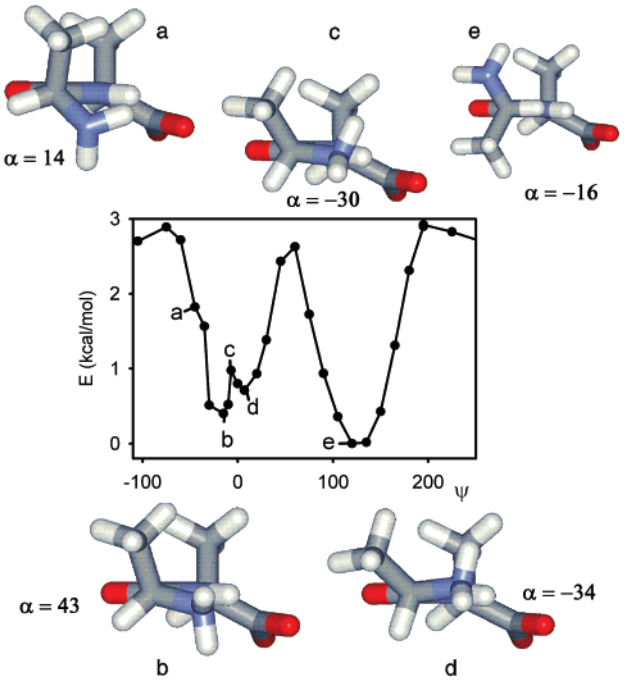

Figure 3. Detailed one-dimensional profile of the AA^- calculated potential energy surface for $\varphi = -150°$. The NH_2 binding pattern changes along the lowest-energy path: (a) the NH_2 hydrogens may be attracted by the COO^- group and the amide bond π-system, or (b) the NH_2 nitrogen electron lone pair creates a hydrogen bond to the amide hydrogen which is (c, d) conserved during the rotation over the syn ($\psi \approx 0°$) conformation. At the other minimum (e), the NH_2 hydrogens are attracted to the π-system as well as to the amide oxygen. The NH_2 rotation is indicated (α, in degrees).

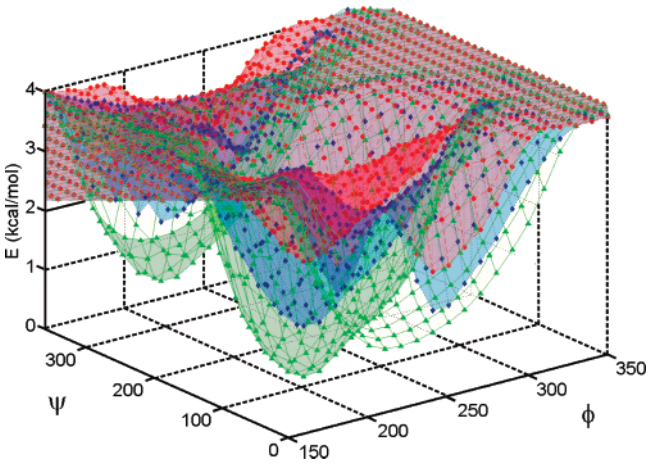

Figure 4. Part of the anionic (AA^-) potential energy surfaces (green, blue, and red) calculated for three NH_2 rotamers.

in AA^- nicely reveals the complexity and caveats that must be taken into account in the modeling of peptide conformational landscape. In longer molecules and proteins the folding of the backbone can presumably be influenced by side-chain interactions similarly as the (ψ, φ) energy map by the NH_2 group rotation. The one- and two-dimensional surfaces (Figures 2 and 3) can be also considered as projections of multidimensional surfaces. Another way illustrating this situation is represented in Figure 4, where three (φ, ψ) anionic surfaces are plotted as obtained from scans with three different NH_2 rotamers. The lowest-energy surface in Figure 2 was obviously obtained by taking the minimum energies for each (φ, ψ) pair in Figure 4.

However minor the purely electrostatic influence of the charged ends on the conformation might be in comparison with the role of the NH_2 group, a more detailed look at the optimal geometries in Table 1 reveals effects that can be attributed solely to the charge/pH changes. The protonation of the COO^- group ($AA^{ZW} \rightarrow AA^+$) results in a change of the φ torsion around the adjacent C−N bond by about 30° with the ψ torsion remaining nearly unaffected. Similarly, for the anionic form the ψ torsion decreases by about 20° under the $NH_3^+ \rightarrow NH_2$ deprotonation of the zwitterion. Whereas the effects of the pH and the NH_2 intrinsic hydrogen bonding can hardly be separated, the charge change undoubtedly further tweaks the dipeptide conformational properties.

Strictly speaking, two rotamers of the COOH group (and two other rotamers associated with the OH rotation are theoretically possible) should be considered in the potential energy surface of the cation AA^+ in a similar way as the NH_2 rotation was treated in the anion AA^-. However, the energy changes involved in the COOH rotation are minor (less than 1 kcal/mol) and so is the effect of these geometry variations on the NMR parameters. Therefore, the AA^+ (φ,ψ) surface was considered only for the lowest-energy COOH conformers.

Not all local minima on the potential energy surfaces in Figure 2 can support a stable quantum state. For both AA^+ and AA^-, only the two lowest-energy conformers are stable. This can be deduced from the two-dimensional Hamiltonian and the resultant localized wave functions shown for the cation and anion in Figure 5. A similar result was obtained for the AA zwitterion.[11] The transition barriers are clearly high enough to support at least the two distinct conformers with the wavefunctions plotted by the green lines in Figure 5. Moreover, we can deduce from the lifetimes of the second-lowest energy states listed in the footnotes of Table 1 (a few milliseconds) that it is in principle possible to prepare these conformers, although presently they cannot be detected by the inherently slow NMR experiment.

By comparison of the computations performed in a vacuum and with the solvent correction (the left- and right-hand parts of Figure 2, respectively), one can well estimate the effect of the environment on the peptide conformational properties. While it is true that the basic conformational characteristics of the dipeptide given by the covalent bonds do not change upon the solvation, the final energy profiles, the exact minima geometries, and, particularly, the steepness of the equilibrium potential wells do change. The MP2 method provides virtually the same conformers as the BPW91 functional (Table 1) except for the φ angle of the AA^+ form; in this case, however, the global minimum well is very broad and the equilibrium φ difference does not necessarily implicate a different behavior. Other backbone torsion angles obtained for the minima with the BPW91 and MP2 methods differ by less than 6°. The values of the torsion angles for the **A**-type AA conformers are close to those observed in β-sheet structures of longer peptides and proteins (antiparallel β-sheet: $\varphi,\psi = -139°,135°$; parallel β-sheets: $\varphi,\psi = -119°,113°$),[29] whereas the other types do not have canonical protein counterparts.

Similarly as for the zwitterion,[11] molecular dynamics (MD) simulations provided analogous conformer distribution to those deduced from the ab initio relative energies also for the positively and negatively charged AA forms (see Figure 1s in SI for the Amber force field). Particularly, the MD computations are consistent with the one (for AA^{ZW} and AA^+) and two (for AA^-) conformer presence in the sample under room temperature. Obviously, detailed MD results strongly depend on the force field parametrization, and presently we consider them inferior to those based on the DFT energy maps.

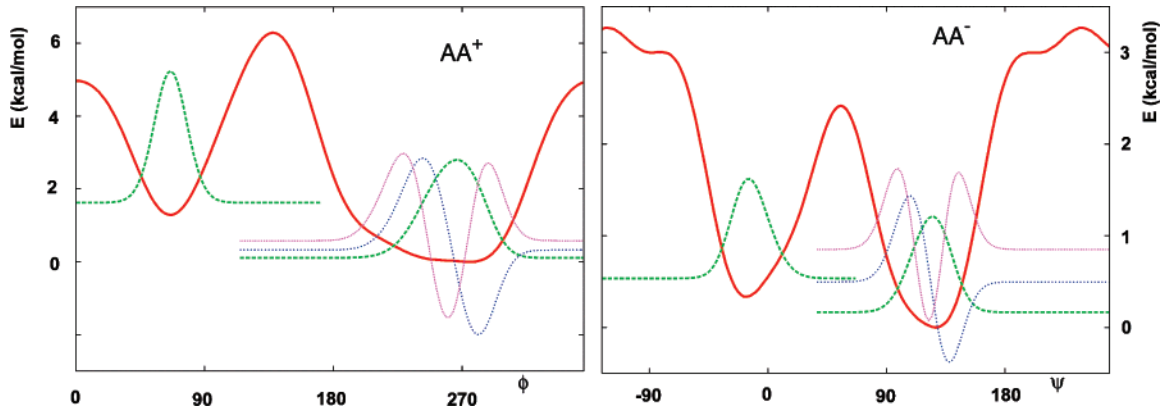

Figure 5. One-dimensional sections of the cation (AA^+) and anion (AA^-) smoothed potential energy surfaces (the red line) and vibrational wave functions of the lowest-energy states (the dashed/dotted lines, with the asymptotes corresponding to their energies).

TABLE 2: Experimental (in D_2O) and Computed[a] Changes of Alanine NMR Parameters under the pH Variations

	$\Delta(A^+ - A^{ZW})$		A^{ZW}		$\Delta(A^- - A^{ZW})$	
	calcd	exptl	calcd	exptl	calcd	exptl
			Chemical Shifts (ppm)			
N	−4.00	−2.20	−386.1	−339.6	−13.1	−6.6
C2	−0.17	−1.77	62.79	53.35	1.32	0.93
C3	−0.26	−3.11	188.38	178.66	11.74	8.94
C4	−0.27	−0.83	20.70	18.97	8.14	4.25
H2	0.81	0.37	4.17	3.78	−0.64	−0.48
H4	0.18	0.08	1.57	1.48	−0.44	−0.26
			Spin−Spin Coupling Constants (Hz)			
^1J:						
N1,C2	−1.6	−0.85	−3.2	−5.7	1.9	1.4
C2,C4	−4.1	−0.8	36.8	34.9	−1.9	0.3
C2,C3	12.2	5.6	48.5	54.0	3.1	−1.3
C2,H2	4.4	1.5	143.6	145.1	−10.4	−6.7
C4,H4	2.9	1.3	127.0	129.7	−3.4	−2.1
^2J:						
N1,H2	−0.2	0	−0.9	0	−2.4	−2.2
N1,C4	−0.1	0	−0.7	0	−3.1	0
N1,C3	0.1	0	−0.5	0	0	0
C2,H4	0.2	−0.2	−3.1	−4.4	0.3	0.1
C4,H2	−0.8	−0.35	−3.1	−4.55	1.0	−0.15
C3,C4	−0.3	−0.1	−0.7	−1.2	0.4	1.2
C3,H2	−0.8	−1.0	−4.6	−5.0	0.5	0.7
^3J:						
N1,H4	0.3	0.05	−3.3	−3.05	0.6	0.1
C3,H4	0.5	0.35	4.1	4.2	−0.2	0.1
H2,H4	0.1	0	7.3	7.3	−0.6	−0.2

[a] BPW91/6-311++G**/PCM geometries, B3LYP/IGLOIII NMR parameters. For A^+ and A^-, differences with respect to A^{ZW} are given; for A^-; the values calculated for three NH_2 rotamers were averaged.

Alanine NMR pH Dependence. The anion (A^-), cation (A^+), and zwitterion (A^{ZW}) of the ^{15}N,^{13}C-isotopically labeled alanine allowed us to investigate the dependence of the chemical shifts and spin−spin coupling constants for a system where no significant change of molecular shape can be induced by the change of the molecular charge. A complete set of experimental and calculated NMR parameters is given in Table 2. The absolute chemical shifts are reproduced with a notable error (e.g., computed 53.35 ppm, experimental 62.79 ppm for C2); nevertheless all signs of the differences between the charged and neutral forms are reproduced correctly. As expected, the hydrogen shifts could be calculated with a higher precision than those for the heavy atoms.

The alanine spin−spin coupling constants change under the deprotonation and protonation like the shifts, typically within 1−10%. The computation well reproduces the magnitudes of the individual coupling constants (e.g., for A^{ZW}, the experimental ^1J(C2,H2) = 145.1 Hz was calculated as 143.6 Hz, i.e., with 1% error). As in the case of the shifts, the computations reproduce most trends induced by the pH change, albeit with a limited precision. As an extreme case, the ^1J(C2,C3) coupling changes by −1.3 Hz while a +3.1 Hz change is predicted by the theory. With the exception of the error of the DFT method, we attribute the deviations to MD or solvent−solute interactions, incompletely covered by the present model. Other functionals (BPW91) and bases (IGLOII, 6-311++G**) provided similar results. Overall, we can see that the computations correctly reproduce the main changes in NMR shifts and coupling patterns induced by the change of molecular charge.

Accuracy of the Calculated NMR Parameters in AA. For the AA^+ cation, the accuracy of various approximate levels used for the computations of the NMR shifts and coupling constants are demonstrated in Table 3. The anion AA^- behaves similarly; the data can be found in the SI (Table 1s). As for alanine, the error of the chemical shifts computed for dialanine significantly exceeds the estimated experimental inaccuracy (estimated as 0.01, 0.02, and 4 ppm for the NMR shifts of hydrogen, carbon, and nitrogen, respectively). As observed earlier,[11,30] the hydrogen shifts are reproduced relatively accurately, whereas the DFT method becomes inaccurate for carbons, with the inaccuracy being even higher for the nitrogen atom. The parameters computed at different approximation levels do not vary dramatically. The best overall agreement of the calculated data with the experiment was achieved with the BPW91/6-311++G**/PCM equilibrium geometry and at the B3LYP/IGLOII/PCM level for the NMR parameters. The IGLOIII basis, although bigger, provides less accurate shifts than IGLOII.

Interestingly enough, the gas-phase computations appear to be reasonably accurate. For the geometry obtained with the MP2 method in the gas phase (vacuum), for example, the calculated carbonyl carbon shifts are even closer to experiment than when the PCM solvent correction is applied. For DFT, however, the PCM results are more precise. The differences in geometries (Table 1) and NMR shifts obtained with the MP2 and DFT and with PCM and gas phase might indicate that the current potential energy surfaces (Figure 2) are not quite accurate and that a better solvent model accounting for the directional hydrogen bonds[31] would be more appropriate; this is, however, impossible to achieve with the computer means available. On the other hand, some properties of the dipeptide are reproduced very well, e.g., the observed 84 ppm shift difference between N1 and N4 was calculated within the 92−95 ppm interval. The chemical environment (amine−amide) is thus perhaps more reproducible than solvent environment (vacuum−water), whose influence is weaker.

TABLE 3: Chemical Shifts and Spin−Spin Coupling Constants Calculated at Different Levels of Theory for Conformer A of the AA^+ Cation[a]

geometry (6-311++G**): NMR (B3LYP):	BPW91 PCM IGLOIII/PCM	BPW91 PCM IGLOII/PCM	BPW91 (gas) IGLOIII (gas)	MP2 PCM IGLOIII/PCM	MP2 (gas) IGLOIII (gas)	exptl
			Chemical Shifts (ppm)			
H2	4.63	4.45	4.07	4.40	3.87	4.10
H5	5.53	5.27	4.75	5.01	4.58	4.42
H7	1.58	1.58	1.77	1.41	1.56	1.55
H8	1.48	1.45	1.69	1.31	1.52	1.45
C2	63.2	61.4	63.3	59.9	60.0	51.8
C3	182.6	177.4	178.7	181.5	176.0	173.5
C5	56.4	54.6	61.8	55.7	58.9	51.6
C6	192.2	186.6	187.9	189.8	185.7	179.1
C7	22.0	21.5	21.0	21.8	22.2	19.4
C8	24.3	23.8	21.8	23.2	21.4	18.9
N1	−390	−379	−390	−392	−392	−342
N4	−295	−288	−297	−300	−299	−258
$\Delta\sigma$	11.09	8.27	10.67	10.89	10.11	
			Coupling Constants (Hz)			
^1J:						
C7,H7	129.1	129.8	130.2	128.6	129.9	130.7
C8,H8	128.7	129.3	130.7	128.1	129.8	130.4
C5,H5	140.1	141.8	144.6	142.1	144.1	146.8
C2,C3	52.1	54.5	45.4	51.9	46.1	52.4
C5,C6	60.6	63.7	58.7	60.1	58.6	58.9
C2,C7	32.7	34.6	33.7	32.0	31.8	33.7
C5,C8	33.7	35.6	32.6	32.2	32.1	34.4
C2,N1	−4.6	−5.0	−6.0	−0.2	−0.6	−9.2
C3,N4	−18.4	−19.4	−23.0	−18.4	−22.5	−17.0
C5,N4	−11.8	−12.6	−10.8	−12.3	−11.3	−11.5
^2J:						
C2,H7	−2.6	−3.2	−2.6	−2.8	−2.6	−4.4
C5,H8	−2.9	−3.5	−2.9	−3.0	−3.0	−4.5
C7,H2	−2.6	−3.0	−2.8	−2.5	−2.4	−3.9
C8,H5	−4.7	−5.0	−3.8	−4.1	−3.7	−4.2
C6,H5	−6.2	−6.9	−5.7	−6.3	−5.7	−4.2
C6,C8	0.2	0.1	−1.2	−0.6	−1.3	1.1
C7,N1	−0.5	−0.5	−0.4	−0.5	−0.5	1.3
C2,N4	−11.1	−11.6	−8.5	−11.0	−9.2	−6.9
C6,N4	−1.0	−1.0	−1.1	−1.2	−1.0	−1.1
^3J:						
H2,H7	7.0	6.7	7.2	6.9	7.2	7.1
H5,H8	7.3	7.1	7.0	7.2	7.1	7.0
C3,H7	4.3	4.4	4.6	4.2	4.3	4.4
C6,H8	4.4	4.5	4.7	4.4	4.6	4.5
N1,H7	−3.8	−3.8	−3.7	−3.8	−4.0	−3.1
N4,H8	−2.8	−2.8	−2.9	−2.5	−2.9	−3.1
C2,C5	2.4	2.5	2.2	2.5	2.2	2.1
ΔJ	1.4	1.5	1.4	1.6	1.7	

[a] $\Delta\sigma$ and ΔJ are average absolute deviations. Isotropic shielding values of (31.83, 183.45, and −180.16 ppm, for the H, C, and N atoms, respectively) and (31.53, 181.10, and −194.36 ppm) were used for the IGLOII and IGLOIII computations.

The scalar couplings calculated using different approaches (the lower part of Table 3) also vary rather moderately. Like the shifts, the average absolute deviations ranging in a narrow interval of 1.4−1.7 Hz do not favor any particular method. No preferential approach was indicated even by a decomposition of the statistics into the absolute average deviations for the ^1J, ^2J, and ^3J couplings (not shown). The final precision seems to be an internal property of the B3LYP functional and perhaps the DFT methodology;[32] it was also discussed in previous works.[11,33] An occasional generalization, however, can be made. Particularly, the application of the PCM method improves some one-bond couplings (^1J(C2,C3) and ^1J(C3,N4)) for both the DFT and MP2 geometries. On the contrary, some couplings deviate more from the experiment upon the application of PCM (^2J(C2,N4) and ^1J(C5,H5)). As expected, the charged and polar groups are the most sensitive to the PCM−vacuum environment change.

Behavior similar to that of the calculated cation chemical shifts was also observed for the anion (Table 1s in the SI), although here the situation is complicated by the influence of the NH_2 group rotation. Indeed, a relatively large dispersion of the calculated shifts appeared for the nuclei in the vicinity of the amine group. For the three NH_2 rotamers of the conformer **A**, the calculated shifts are, for example, 24.7, 24.7, and 29.5 ppm for carbon C7, 63.3, 63.9, and 63.7 ppm for carbon C2, and 193.8, 190.7, and 190.6 ppm for carbon C3. The dispersion is even bigger for the conformer **C**: 27.1, 25.9, and 25.7 ppm for carbon C7, 61.9, 62.9, and 65.5 ppm for carbon C2, and 190.4, 191.5, and 193.7 ppm for carbon C3.

AA Chemical Shifts. Similarly as for the alanine, the computed and experimental chemical shift changes for the charged AA forms (related to AA^{ZW}, Figure 6) confirm that the theory can reproduce the experiment on average but with a limited accuracy. Extreme changes are usually better reproduced than the small ones. Especially the hydrogen shift changes are smaller than 0.5 ppm, with the exception of H1 (experimental values are σ = 6.16 ppm for AA^{ZW} and 8.09 ppm for AA^+)

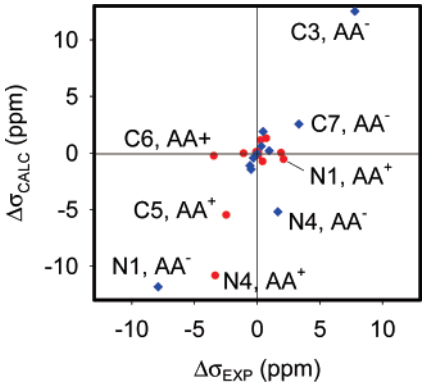

Figure 6. Comparison of calculated and experimental pH chemical shift changes (for the lowest-energy AA^+ and AA^- conformers, with respect to the zwitterionic form AA^{ZW}). For the biggest changes, the corresponding atoms are indicated in the plot.

and not easily reproducible. The amide NH group is also problematic: the computation overestimates the observed nitrogen (N4) shift both in the anion and cation. On the other hand, the amide carbon (C3) change in AA^- is easily reproduced; it is clearly caused by the loss of charge at the amine group. Large charge-induced shift variations (exceeding 1 ppm) have also been measured for the C5, C6, and N1 AA^+ atoms, all indicated in Figure 6. The calculated carbon shifts (conformer **A** in cation, zwitterion, and anion) of C3 (182.6, 181.3, 193.8 ppm), C5 (56.4, 61.9, 60.5 ppm), C6 (192.2, 192.5, 194.4 ppm), and C7 (19.4, 19.3, 22.6) thus nicely correspond to the trend observed under the pH change experimentally: C3 (173.5, 172.8, 180.6 ppm), C5 (51.6, 54.1, 53.6 ppm), C6 (179.1, 182.5, 183 ppm), and C7 (22.0, 22.2, 24.7 ppm). This reflects a general tendency of the ab initio/DFT computation to reproduce relative values of NMR parameters with a higher accuracy than for absolute ones.[34]

The accuracy of the calculated shifts (Table 2s in Supporting Information), however, is not sufficient to discriminate between the individual AA conformers **A**−**F**. For example, the absolute overall deviations from the experiment range within 11.1−11.7, 11.8−16.5, and 11.3−11.9 ppm (for the cation, zwitterion, and anion, respectively) only. All three AA forms thus behave similarly. The variations of the calculated NMR shifts should then be attributed to several factors, such as the reaction of the PCM continuum to the charge redistribution in the charged peptide forms, and do not directly reflect detailed conformational changes.

AA Spin−Spin Coupling. As documented in Figure 7, the coupling constant pH variation can be reproduced with the computation similarly as the shifts. Also here, smaller changes are less reliably calculated than the bigger ones, and the theoretical values concerning the vicinity of the charged residues are less accurate. The change of ^1J(C5,H5) in AA^+, for example, was predicted at the opposite direction. The magnitudes of the one-bond (^1J) constants change most, but the biggest relative changes can be found between the vicinal and geminal couplings (^2J,^3J).

Unlike for the shifts, calculated coupling constants provide useful information on AA conformation. This can be seen for the anion AA^- in Table 4, where the measurable coupling constants calculated for 10 conformers are listed and compared to the experiment. We can see that the results are consistent with the estimated relative conformer energies: The coupling constants calculated for the energetically inconvenient conformers (**B**, **D**−**F**) significantly deviate from the experimental values, which is also indicated by the average absolute deviations from the experiment listed at the bottom of the Table. The conformer **C** alone exhibits the lowest average deviations in the constants, whereas the **A** conformer is more preferred energetically. However, this can be explained by the conformational equilibrium. Indeed, the Boltzmann averaging, taking into account all the conformers **A**−**F** including the NH_2 group rotamers, provides a reasonably low average deviation of the couplings. Obviously, as discussed above and observed in previous works,[11,33] a future improvement of the computational model is desirable because more accurate theoretical constants can lead to a better discrimination between the peptide conformers.

For example, the NMR spectra would be sensitive to the NH_2 group rotation as the constants computed for the three rotamers differ significantly (for conformer **A**, the calculated ^1J(C2,H2) are 135.9, 134.0, and 136.8 Hz, ^1J(C2,C3) 48.3, 53.4, and 53.4 Hz, ^2J(N1,H2) −3.3, 0.7, and −3.9 Hz, etc.). The NH_2 rotation, however, influences the couplings only locally with remote atomic groups not being affected: The constants ^1J(N4,H4)

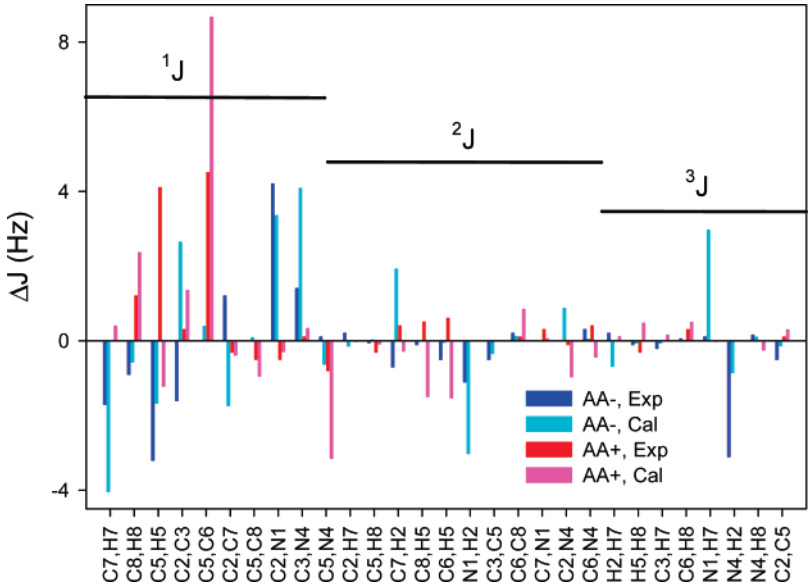

Figure 7. Computed and experimental pH-induced changes of spin−spin coupling constants (for the lowest-energy conformer of AA^+ and AA^-, with respect to that of the zwitterionic form AA^{ZW}).

TABLE 4: Spin−Spin Coupling Constants (Hz) Calculated for 10 AA^- Conformers (A−F)[a] and Comparison with Experimental Values

	A	A′	A″	B	C	C′	C″	D	E	F		
η[b]	0.452	0.119	0.018	0.000	0.240	0.125	0.041	0.000	0.005	0.000	avg[c]	exptl[d]
J^1:												
C7,H7	125.0	124.7	125.0	125.0	125.5	124.9	125.5	124.9	123.9	123.7	125.0	129.0
C8,H8	125.8	125.8	125.7	125.0	125.7	125.6	125.8	124.8	125.9	125.1	125.7	128.3
C2,H2	135.9	136.8	134.0	135.4	137.7	130.6	137.8	130.5	136.2	135.1	135.7	142.2
C5,H5	139.6	139.6	139.5	127.6	139.2	138.8	139.6	127.6	140.1	127.6	139.4	139.5
C2,C3	48.3	53.4	53.4	47.8	52.5	52.6	47.1	52.5	48.8	48.2	50.5	50.5
C5,C6	52.3	52.3	52.4	52.3	52.5	52.4	52.1	52.5	51.3	52.4	52.3	54.4
C2,C7	36.5	31.3	35.9	36.0	34.0	35.3	35.2	35.6	36.6	36.6	35.0	35.2
C5,C8	34.6	34.7	34.6	39.2	34.6	34.9	35.0	39.0	35.2	39.2	34.7	34.9
C2,N1	−1.2	−1.0	−2.6	−1.2	−2.6	−2.0	−1.2	−2.2	−0.7	−0.8	−1.6	−4.5
C3,N4	−13.6	−14.6	−14.5	−13.8	−16.0	−15.9	−15.4	−16.7	−13.7	−13.9	−14.7	−15.7
C5,N4	−9.2	−9.3	−9.3	−9.0	−9.9	−9.9	−9.6	−9.8	−9.3	−9.1	−9.5	−10.6
J^2:												
C2,H7	−2.8	−2.8	−2.8	−2.8	−2.9	−3.1	−2.9	−3.1	−2.9	−3.0	−2.9	−4.2
C5,H8	−2.8	−2.8	−2.8	−3.3	−2.8	−2.8	−2.8	−3.3	−2.9	−3.3	−2.8	−4.25
C7,H2	−3.3	−0.4	−0.8	−3.5	−3.1	−3.5	−4.8	−3.8	−2.9	−3.1	−3.0	−5.0
C8,H5	−3.2	−3.2	−3.2	−3.8	−3.2	−3.2	−3.2	−3.5	−3.0	−3.8	−3.2	−4.8
C3,H2	−1.1	−3.9	−0.8	−1.1	−3.2	−6.1	−3.6	−5.9	−4.5	−4.2	−2.7	−5.0
C6,H5	−4.7	−4.7	−4.7	−5.9	−4.6	−4.6	−4.7	−5.9	−4.6	−5.9	−4.7	−5.3
N1,H2	−3.3	−3.9	0.7	−3.3	1.2	−1.2	−4.4	−0.7	−2.4	−2.4	−2.0	−1.1
C3,C5	−0.9	−0.6	−0.5	−0.8	−0.3	−0.3	−0.5	−0.1	−1.0	−0.9	−0.6	−0.5
C6,C8	−0.6	−0.6	−0.5	0.7	−0.6	−0.5	−0.5	0.7	−0.8	0.6	−0.6	1.2
C2,N4	−9.1	−9.3	−9.6	−9.3	−6.6	−6.4	−7.5	−6.5	−7.8	−7.6	−8.1	−6.8
C6,N4	−0.5	−0.5	−0.5	0.2	−0.7	−0.6	−0.6	0.2	−0.6	0.2	−0.6	−1.2
J^3:												
H2,H7	6.7	6.2	6.2	6.8	6.8	6.8	7.1	6.9	7.0	6.9	6.7	7.3
H5,H8	6.8	6.8	6.8	7.0	6.8	6.9	6.8	7.0	6.8	7.0	6.8	7.2
C3,H7	4.1	4.1	4.5	4.0	4.3	3.9	4.0	4.0	4.0	4.0	4.1	4.2
C6,H8	3.9	3.9	3.9	3.5	3.9	3.9	3.9	3.5	4.0	3.5	3.9	4.25
N1,H7	−3.7	−0.8	−3.4	−3.7	−2.9	−1.0	−3.7	−1.1	−3.8	−3.7	−2.8	−3.0
N4,H2	−0.8	−1.2	−1.2	−0.7	−0.7	−0.6	−1.1	−0.4	−1.2	−1.1	−0.8	−2.1
N4,H8	−2.5	−2.5	−2.5	−2.5	−2.5	−2.5	−2.5	−2.4	−2.5	−2.5	−2.5	−2.95
C2,C5	1.7	2.0	2.0	2.1	1.3	1.3	1.4	1.7	1.3	1.6	1.6	1.5
ΔJ[e]	1.6	1.7	1.7	2.1	1.2	1.4	1.2	1.9	1.5	2.0	1.3	0.0

[a] See Table 1 for the definition of the conformers. [b] Conformer ratios were estimated from the Boltzmann factor at 300 K. [c] The Boltzmann-weighted average. [d] pH = 12. [e] Average absolute deviations.

(−91.5, −91.4, and −91.6 Hz for the three rotamers), ^2J(C5,H4) (3.2, 3.2, and 3.1 Hz), or ^3J(H4,H5) (7.1, 7.4, and 7.2 Hz) are rather insensitive to the rotation.

Also the computed coupling constants of the AA^+ form listed in Table 5 agree best with the experiment for the energy-preferred conformer **A**. Average deviations of the **C** conformer are low as well, but this form can be excluded on the basis of the energy estimation. For the cation, especially the vicinal couplings (^3J) seem to be computed with significant errors. Fortunately, for AA^+, the number of conformers that can contribute to the averaged observed J's is smaller than for AA^-. In fact, the conformer **A** seems to be clearly dominant (∼90%), with Boltzmann population of the conformer **B** estimated from the equilibrium geometry being about 10%. Given the narrow potential well (Figure 2) in comparison with **A**, the population of conformer **B**, obtained through a complete integration over the two-dimensional potential energy surface, would be even smaller. Additionally, the average error ($\Delta J = 1.9$ Hz, see Table 5) of the couplings for the **B** form is much higher than that for **A** ($\Delta J = 1.4$ Hz).

Finally, we can focus our attention on the conformational sensitivity of individual spin−spin coupling constants represented by the average absolute deviations plotted in Figure 8. In spite of the errors of the computed couplings, some constants clearly exhibit larger variations under the conformational change, and thus the NMR technique along with the quantum computation may be able to discriminate between peptide conformers. The ^1J(C5,H5) coupling is the most sensitive one, particularly to the change of the close φ angle, and can thus monitor the ratios of the (**A**, **C**) and (**B**, **D**) conformer classes (cf. Tables 4 and 5). The ψ torsion has little impact on this coupling. Similarly, the analogous ^1J(C2,H2) coupling constant is more sensitive to the ψ angle, which makes it possible for these two couplings alone in principle to determine the AA secondary structure. To be able to generalize the results, however, one has to realize also the dependence on the molecular charge (the experimental ^1J(C5,H5) constant is 146.8, 142.7, and 139.5 Hz for the cation, zwitterion, and anion, respectively), and in larger peptides similar variation can be expected for various amino acid side chains. The ^1J(C5,C6) coupling, for example, is predominantly driven by the molecular charge (the measured values for the cation, zwitterion, and anion are 58.9, 54.4, and 54.4 Hz, which are actually very well reproduced by the calculation as 60.6, 51.9, and 52.3 Hz; see Tables 4 and 5 and ref 11), and the conformational variance does not exceed 0.7 Hz.

The three-bond couplings, however, are more important for the peptide structural determination than the one- and two-bond interactions.[1,2,12,13] Therefore, their dependence on other factors than the torsion angle, such as charges of close molecular groups, is of paramount importance for peptide chemistry. As an example, two constants, ^3J(H4,H5) and ^3J(N4,H2), were selected and their dependence on the main-chain torsion angle plotted in Figure 9. Calculated curves for the AA cation, anion, and zwitterions are compared to the empirical Karplus-type curves derived in the literature on the basis of theoretical and

TABLE 5: Spin−Spin Coupling Constants (Hz) Calculated for Four AA^+ Conformers and a Comparison with the Experiment[a]

	A	B	C	D	
η	0.91	0.09	0.00	0.00	exptl
^1J:					
C7,H7	129.1	129.2	128.9	128.9	130.7
C8,H8	128.7	127.7	128.7	127.5	130.4
C5,H5	140.1	132.5	140.8	133.2	146.8
C2,C3	52.1	51.1	54.6	53.4	52.4
C5,C6	60.6	59.2	60.8	59.5	58.9
C2,C7	32.7	32.7	32.1	32.2	33.7
C5,C8	33.7	38.9	33.5	39.1	34.4
C2,N1	−4.6	−4.6	−0.7	−0.8	−9.2
C3,N4	−18.4	−17.6	−16.4	−15.6	−17.0
C5,N4	−11.8	−9.4	−11.8	−9.1	−11.5
^2J:					
C2,H7	−2.6	−2.6	−2.5	−2.5	−4.4
C5,H8	−2.9	−3.3	−2.9	−3.3	−4.5
C7,H2	−2.6	−2.7	−3.1	−3.1	−3.9
C8,H5	−4.7	−4.2	−4.7	−3.9	−4.2
C6,H5	−6.2	−7.2	−6.3	−6.8	−4.2
C6,C8	0.2	1.1	0.1	1.1	1.1
C7,N1	−0.5	−0.5	−0.4	−0.4	1.3
C2,N4	−11.1	−10.9	−8.7	−8.5	−6.9
C6,N4	−1.0	0.3	−1.2	0.5	−1.1
^3J:					
H2,H7	7.0	7.0	7.2	7.2	7.1
H5,H8	7.3	7.0	7.3	6.9	7.0
C3,H7	4.3	4.2	4.5	4.4	4.4
C6,H8	4.4	4.5	4.4	4.5	4.5
N1,H7	−3.8	−3.8	−4.1	−4.1	−3.1
N4,H8	−2.8	−2.6	−2.7	−2.7	−3.1
C2,C5	2.4	2.6	1.3	1.5	2.1
ΔJ	1.4	1.9	1.5	2.0	

[a] The symbols have the same reference as in Table 4.

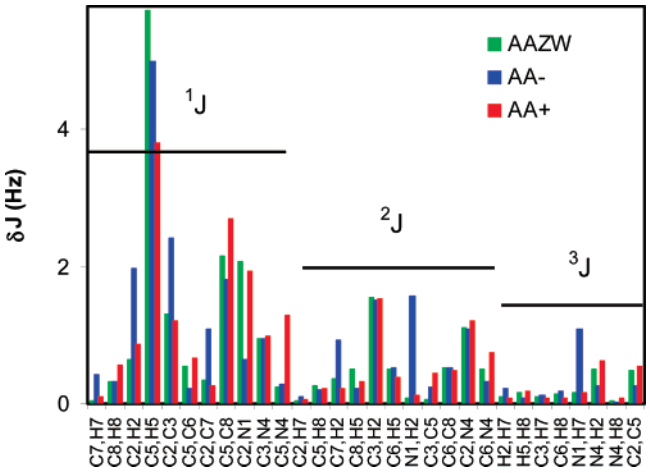

Figure 8. Computed sensitivities of selected spin−spin coupling constants to the conformational change (average absolute deviations from the average over individual conformers **A**−**F** are plotted for each form).

experimental data. Clearly, for ^3J(H4,H5), the angular dependence does not rely significantly on the molecular charge and nicely corresponds to the two approximations proposed previously. Within $\varphi \approx -180...-30°$, the cationic AA^+ ^3J(H4,H5) curve somewhat deviates from the anion and zwitterion, which can be explained by the vicinity of the COO^- group, protonated in the cation. Some dispersion occurs also around $\varphi \approx 150°$; this is, however, rather minor with respect to the principal conformational dependence.

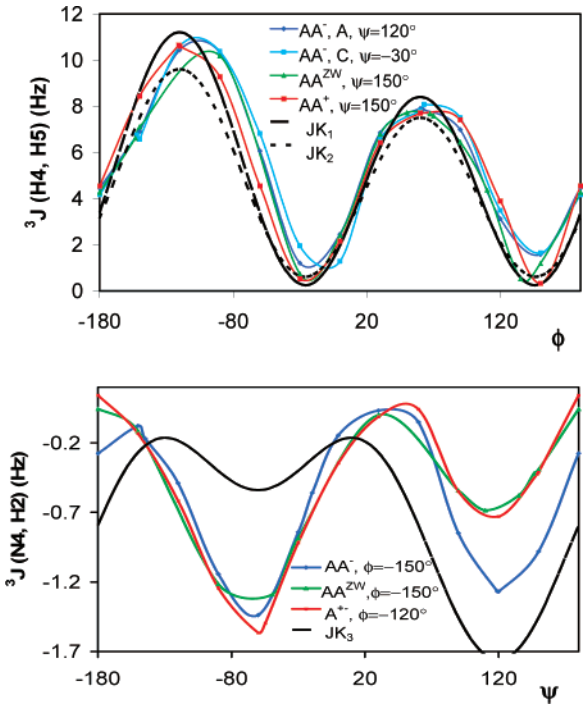

Figure 9. Calculated dependence of the ^3J(H4,H5) (top) and ^3J(N4,H2) (bottom) vicinal spin−spin coupling constants on the encompassed torsion angle for the three charged AA forms and a comparison to the JK_1,[35] JK_2,[36] and JK_3[37] semiempirical Karplus curves.

Apparently, the ^3J(N4,H2) coupling (lower part of Figure 9) is more sensitive to the molecular charge and deviates more from the previously proposed curve. As expected, the anion AA^- curve deviates from the cation and zwitterion because of the deprotonation of the NH_3^+ group close to the rotating bond. However, a closer inspection reveals that the absolute coupling dispersion is like for the previous case, since the ^3J(N4,H2) constant varies in a much narrower range than ^3J(H4,H5).

Conclusions

On the basis of the DFT computations (BPW91/6-311++G**) of the two-dimensional potential energy surfaces, we were able to estimate the conformational behavior of the AA dipeptide under the pH changes. Whereas the neutral zwitterionic form AA^{ZW} and the cation (AA^+) adopt similar conformations of the main peptide chain (φ, ψ angles), the anion (AA^-) exists in two forms differing by the ψ-angle values. The forms are approximately equally populated in aqueous solutions at room temperature. The anion main chain folding is more complex than for the other forms because of the influence of the NH_2 group, which can serve both as a hydrogen donor and acceptor in an intramolecular hydrogen bonding. The results of the analysis of the potential energy surfaces are in agreement with both experimental and calculated NMR chemical shifts and spin−spin coupling constants. The NMR parameters could be calculated with a limited accuracy, but the pH dependence of the chemical shifts for the dipeptide as well as for the alanine monomer could be explained on the basis of the theory. Furthermore, the comparison of the experimental and calculated coupling constants is consistent with the energetic analysis.

Acknowledgment. The work was supported by the Czech Science Foundation (Grant Nos. 203/06/0420 and 202/07/0732), the Grant Agency of the Academy of Sciences (A4005507020, A400550701), and the Ministry of Education, Youth and Sports (Grant No. LC512).

Supporting Information Available: Cartesian coordinates, absolute energies of equilibrium structures, and additional computational and experimental details. This material is available free of charge via the Internet at http://pubs.acs.org.

References and Notes

(1) Kessler, H.; Seip, S. In *Two-Dimensional NMR Spectroscopy, Application for Chemists and Biochemists*; Croasmun, W. R., Carlson, R. M. K., Eds.; VCH Publ.: New York, 1994; p 619.

(2) Wüthrich, K. *NMR of Proteins and Nucleic Acids*; Wiley: New York, 1986.

(3) Englander, S. W.; Mayne, L. *Annu. Rev. Biophys. Biomol. Struct.* **1992**, *21*, 243.

(4) Evans, J. N. S. *Biomolecular NMR Spectroscopy*; Oxford University Press: Oxford, 1995.

(5) William, M. P.; Waltho, J. P. *Chem. Soc. Rev.* **1992**, *21*, 227.

(6) Wolinski, K.; Hilton, J. F.; Pulay, P. *J. Am. Chem. Soc.* **1990**, *112*, 8251.

(7) Sychrovský, V.; Gräfenstein, J.; Cremer, D. *J. Chem. Phys.* **2000**, *113*, 3530.

(8) Helgaker, T.; Watson, M.; Handy, N. C. *J. Chem. Phys.* **2000**, *113*, 9402.

(9) Barone, V.; Peralta, J. E.; Contreras, R. H.; Snyder, J. P. *J. Phys. Chem. A* **2002**, *106*, 5607.

(10) Bouř, P.; Sychrovský, V.; Maloň, P.; Hanzlíková, J.; Baumruk, V.; Pospíšek, J.; Buděšínský, M. *J. Phys. Chem. A* **2002**, *106*, 7321.

(11) Bouř, P.; Buděšínský, M.; Špirko, V.; Kapitán, J.; Šebestík, J.; Sychrovský, V. *J. Am. Chem. Soc.* **2005**, *127*, 17079.

(12) Karplus, M.; Weaver, D. L. *Nature* **1976**, *260*, 404.

(13) Perere, S. A.; Bartlett, R. J. *Magn. Reson. Chem.* **2001**, *39*, S183.

(14) Laws, D. D.; deDios, A. C.; Oldfield, E. *J. Biomol. NMR* **1993**, *3*, 607.

(15) Birn, J.; Poon, A.; Mao, Y.; Ramamoorthy, A. *J. Am. Chem. Soc.* **2004**, *126*, 8529.

(16) Ṣebastiani, D.; Rothlisberger, U. *J. Phys. Chem. B* **2004**, *108*, 2807.

(17) Čejchan, A.; Špirko, V. *J. Mol. Spectrosc.* **2003**, *217*, 142.

(18) Frisch, M. J.; Trucks, G. W.; Schlegel, H. B.; Scuseria, G. E.; Robb, M. A.; Cheeseman, J. R.; Montgomery, J., J. A.; Vreven, T.; Kudin, K. N.; Burant, J. C.; Millam, J. M.; Iyengar, S. S.; Tomasi, J.; Barone, V.; Mennucci, B.; Cossi, M.; Scalmani, G.; Rega, N.; Petersson, G. A.; Nakatsuji, H.; Hada, M.; Ehara, M.; Toyota, K.; Fukuda, R.; Hasegawa, J.; Ishida, M.; Nakajima, T.; Honda, Y.; Kitao, O.; Nakai, H.; Klene, M.; Li, X.; Knox, J. E.; Hratchian, H. P.; Cross, J. B.; Bakken, V.; Adamo, C.; Jaramillo, J.; Gomperts, R.; Stratmann, R. E.; Yazyev, O.; Austin, A. J.; Cammi, R.; Pomelli, C.; Ochterski, J. W.; Ayala, P. Y.; Morokuma, K.; Voth, G. A.; Salvador, P.; Dannenberg, J. J.; Zakrzewski, V. G.; Dapprich, S.; Daniels, A. D.; Strain, M. C.; Farkas, O.; Malick, D. K.; Rabuck, A. D.; Raghavachari, K.; Foresman, J. B.; Ortiz, J. V.; Cui, Q.; Baboul, A. G.; Clifford, S.; Cioslowski, J.; Stefanov, B. B.; Liu, G.; Liashenko, A.; Piskorz, P.; Komaromi, I.; Martin, R. L.; Fox, D. J.; Keith, T.; Al-Laham, M. A.; Peng, C. Y.; Nanayakkara, A.; Challacombe, M.; Gill, P. M. W.; Johnson, B.; Chen, W.; Wong, M. W.; Gonzalez, C.; Pople, J. A. *Gaussian 03*, revision C.02; Gaussian, Inc.: Wallingford, CT, 2004.

(19) Becke, A. *Phys. Rev. A* **1988**, *38*, 3098−3100.

(20) Barone, V.; Cossi, M.; Tomasi, J. *J. Comput. Chem.* **1998**, *19*, 404.

(21) Møller, C.; Plesset, M. S. *Phys. Rev.* **1934**, *46*, 618.

(22) Ruud, K.; Helgaker, T.; Bak, K. L.; Jorgensen, P.; Jensen, H. J. A. *J. Chem. Phys.* **1993**, *99*, 3847.

(23) Bouř, P.; Buděšínský, M. *J. Chem. Phys.* **1999**, *110*, 2836.

(24) Becke, A. D. *J. Chem. Phys.* **1993**, *98*, 5648.

(25) Kutzelnigg, W.; Fleischer, U.; Schindler, M. *NMR - Basic Principles and Progress*; Springer: Heidelberg, 1990; Vol. 23.

(26) Podolsky, B. *Phys. Rev.* **1928**, *32*, 812.

(27) Ixaru, L. *Numerical Methods for Differential Equations and Applications*; Reidel: Dordrecht, 1984.

(28) Špirko, V.; Piecuch, P.; Bludský, O. *J. Chem. Phys.* **2000**, *112*, 189.

(29) Creighton, T. E. *Proteins*; New York, 1984.

(30) Fadda, E.; Casida, M. E.; Salahub, D. R. *J. Phys. Chem. A* **2003**, *107*, 9924.

(31) Bouř, P. *J. Chem. Phys.* **2004**, *121*, 7545.

(32) Kümmel, S.; Kronik, L.; Perdew, J. P. *Phys. Rev. Lett.* **2004**, *93*, 213002.

(33) Bouř, P.; Raich, I.; Kaminský, J.; Hrabal, R.; Čejka, J.; Sychrovský, V. *J. Phys. Chem. A* **2004**, *108*, 6365.

(34) *The Encyclopedia of Computational Chemistry*; Schleyer, P. R., Allinger, N. L., Clark, T., Gasteiger, J., Kollman, P. A., Schaefer, H. F., III, Schreiner, P. R., Eds.; John Wiley & Sons: Chichester, 1998.

(35) Case, D. A.; Scheurer, C.; Brüschweiler, R. *J. Am. Chem. Soc.* **2000**, *122*, 10390.

(36) Schmidt, J. M.; Blümel, M.; Löhr, F.; Rüterjans, H. *J. Biomol. NMR* **1999**, *14*, 1.

(37) Demarco, A.; Llinas, M.; Wührich, K. M. *Biopolymers* **1978**, *17*, 2727.